
Article:
Danao, L.A., Eboibi, O. and Howell, R.J. (2013) An Experimental Investigation into the Influence of Unsteady Wind on the Performance of a Vertical Axis Wind Turbine. Applied Energy, 107. 403 - 411. ISSN 0306-2619

https://doi.org/10.1016/j.apenergy.2013.02.012

An Experimental Investigation into the Influence of Unsteady Wind on the Performance of a Vertical Axis Wind Turbine

Louis Angelo Danao[1], Okeoghene Eboibi[2], Robert Howell[3]

Department of Mechanical Engineering

University of Sheffield, Sheffield S1 3JD, U.K

Abstract

An experimental investigation was carried out on a wind tunnel scale vertical axis wind turbine with unsteady wind conditions. The wind speed at which testing was conducted was 7m/s (giving a Reynolds number of around 50,000) with both 7% and 12% fluctuations in wind velocity at a frequency of 0.5Hz. Rotational speed fluctuations in the VAWT were induced by the unsteady wind and these were used to derive instantaneous turbine rotor power. The results show the unsteady power coefficient (CP) fluctuates following the changes in wind speed. The time average of the unsteady CP with a 7% fluctuation in wind velocity was very close to that with steady wind conditions while 12% fluctuations in wind speed resulted in a drop in the mean CP, meaning unsteady winds of such amplitudes are detrimental to the energy yields from these wind turbines. At mean rotational speeds corresponding to tip speed ratios (λ) beyond peak CP, no significant hysteresis was observed for both 7% and 12% fluctuations. However, substantial hysteresis is seen for conditions where mean λ is below peak CP.

Nomenclature

A	rotor frontal swept area, $2RL$	V_{mean}	mean speed of unsteady wind
c	blade chord		
CP	power coefficient	λ	tip speed ratio, $R\Omega/V_\infty$
f_c	characteristic frequency of unsteady wind	λ_{mean}	tip speed ratio corresponding to Ω_{mean}
I_{rig}	rotor rotational mass moment of inertia	ξ	rotor angular acceleration
L	blade length	ρ	air density
N	number of blades	σ	rotor solidity, Nc/R
P_B	blade power (three blades)	Ω	rotor angular speed
P_w	wind power	Ω_{mean}	in unsteady wind, mean of Ω
R	rotor radius		
T_{app}	applied brake torque	HAWT	horizontal axis wind turbine
T_B	blade torque (three blades)	VAWT	vertical axis wind turbine
T_{res}	resistive torque		
V_{wind}	instantaneous wind speed		
V_∞	free stream wind speed		
V_{amp}	amplitude of fluctuation of unsteady wind		

[1] PhD Student, University of Sheffield; Assistant Professor, University of the Philippines.
[2] PhD Student, University of Sheffield; Lecturer, Delta State Polytechnic, Nigeria.
[3] Lecturer in Experimental Aerodynamics, University of Sheffield.

I. Introduction

The use of wind turbines has risen rapidly in recent years because of the potential that they offer for carbon free power generation. Winds are usually unsteady with high levels of turbulence for significant proportions of the time, resulting in air flows characterised by rapid changes in speed and direction. It has been pointed out several times in literature [1-4] that vertical axis wind turbines (VAWT) may be more appropriate for urban applications because of a number of distinct advantages it presents over the conventional horizontal axis wind turbines (HAWT). These advantages include no need to include a yawing mechanism to adjust the rotor to the changing wind direction, ease of maintenance due to the location of the gearbox – generator system at the base of the turbine, as well as potentially better performance in unsteady and skewed wind conditions [5-7].

However, very little work has been carried out into the effects of VAWT performance in unsteady wind conditions. The vast majority of research published (both numerical and experimental) has been with steady wind flows probably because the detailed analyses of blade loading and rotor performance are well established and fairly straightforward. However, there have been a handful of efforts (mostly numerical) that have attempted to provide initial understanding of the VAWT performance in unsteady wind. Earlier attempts to understand the performance of VAWTs in unsteady wind were carried out by McIntosh et al [8, 9] through numerical modelling. The VAWT was subjected to fluctuating free stream of sinusoidal nature while running at a constant rotational speed. An increase in energy extraction was attained using a rotational speed greater than the calculated steady state maximum. The over–speed control technique resulted to a 245% increase in energy extracted. Further improvements in the performance can be attained by using a tip speed ratio feedback controller incorporating time dependent effects of gust frequency and turbine inertia giving a further 42% increase in energy extraction. At low frequencies of fluctuation (0.05Hz) away from stall, the unsteady CP closely tracks the steady CP curve. However at higher frequencies (0.5Hz), the unsteady CP is seen to form hysteresis loops with averages greater than steady predictions.

Hayashi et al [10] examined the effects of gusts on a VAWT by subjecting a wind tunnel scale rotor to a step change in wind velocity. Two types of control were implemented: constant rpm and constant load torque. When subjected to a step change in wind speed from 10m/s to 11m/s under constant rpm control, the VAWT torque was observed to respond almost instantaneously and attained a steady state in less than 3s. However when constant load torque control was employed, the initial response is similar to the constant rpm control where the torque instantly jumps to a higher level. The subsequent behaviour is a combination of a gradual increase in rpm with a slow decrease in torque until steady state is attained. Despite an observed transient VAWT response that does not follow steady state power curves, they contend that the adopted step change in wind speed is not normally observed in the real world and most likely a more gradual increase is expected. The VAWT behaviour will thus follow a quasi–static condition during the gust.

In 2010, Kooiman and Tullis [11] experimentally tested a VAWT within the urban environment to assess the effects of unsteady wind on aerodynamic performance. Temporal variation in speed and direction was quantified and compared to a base case wind tunnel performance. Independence of the performance in directional fluctuations was seen while amplitude–based wind speed fluctuation decreased the performance linearly. For their particular urban site, the degradation in performance was deemed minimal.

Danao and Howell [12] conducted CFD simulations on a wind tunnel scale VAWT in unsteady wind inflow and have shown that the VAWT performance generally decreased in any of the tested wind fluctuations. The amplitude of fluctuation studied was 50% of the mean wind speed and three sinusoidal frequencies were tested: 1.16Hz, 2.91Hz, and 11.6Hz where the fastest rate is equal to the VAWT rotational frequency. The two slower frequencies of fluctuation showed a 75% decrease in the wind cycle mean performance while the fastest rate caused a 50% reduction. Closer investigation revealed that for a 2.91Hz fluctuation rate a large hysteresis is seen in the unsteady CP of the VAWT within one wind cycle. This hysteresis occurs in the positive amplitude portion of the wind fluctuation where the blades passing the upwind progressively stall at earlier azimuths and experience very deep stall due to significant reduction in the effective λ. Negative amplitude in wind fluctuation does not produce significant hysteresis. However, the unsteady CP traces a curve that does not follow the steady CP curve but somehow crosses it down to a lower level performance curve.

Following the work of Hayashi in 2009, Hara et al [13] studied the effects of pulsating winds on a VAWT and the dependence of the performance to changes in the rotor's moment of inertia. The fluctuating wind was not sinusoidal but alternating gusts and lulls that were equally distant from a mean wind speed. This was implemented by a blade pitch–controlled fan blowing to an Eiffel–type wind tunnel with the rotor 1.5m from the tunnel outlet. Results show a phase delay in the response of the rotational speed from the wind variation but held a constant value of about $\pi/2$ regardless of amplitude. This was explained as an effect of the distance of the VAWT from the tunnel outlet where the hotwire was installed. The energy efficiency of the VAWT was observed to be constant in changing rotor moment of inertia and fluctuation frequency but a decrease is seen when fluctuations have large amplitudes. Further work for a larger scale VAWT using numerical techniques confirm their experimental observations and a locus of torque is produced as the VAWT response to the cyclic changes in wind speed.

In 2012, Scheurich and Brown [14] published their findings on a numerical model of VAWT aerodynamics in unsteady wind conditions. The fluctuating wind had a mean speed of 5.4m/s with a fluctuating frequency of 1Hz. Different fluctuation amplitudes were investigated for three blade configurations: straight, curved, and helical. Constant rotational speed was used in the numerical simulations and the boundary extents were far enough for the model to be considered as open field. Both straight and curved blades exhibited considerable variation in blade loading which is also observed in steady wind results. These variations in CP over one revolution are more significant than those induced by the unsteadiness of the wind. Helical blades perform

much better with the unsteady CP tracing the steady performance curve quite well. Overall performance degradation is observed when fluctuation amplitudes are high while the effect of frequency is minor for practical urban wind conditions. Hysteresis loops of the CP are seen on the helical configuration that extend beyond the steady CP variation especially for the high frequency of wind fluctuation.

The conflicting conclusions from previous published research suggest that very little is still understood about the performance and aerodynamics of VAWTs in unsteady winds. Any generalisations made about VAWT performance in the urban environment may well be completely erroneous.

The research presented with unsteady wind conditions are, to the Authors' knowledge, the first experiments of their kind and the paper will further the understanding of VAWT performance in unsteady wind conditions.

II. Experiment Methods

Wind Tunnel Facility

The wind tunnel used for these experiments was the University of Sheffield – Department of Mechanical Engineering's low–speed wind tunnel. The tunnel is an open-circuit suction type with an axial fan located at the outlet (Figure 1). The wind tunnel has a total length of 8.5m, including the 3m long test section. At the inlet, a honeycomb mesh straightens the inlet flow and breaks up any large scale flow structures present in the room. A series of fine meshes and a settling section permit turbulence and non-uniformities to dissipate, after which the flow is accelerated by a 6.25:1 contraction cone leading to the 1.2m high by 1.2m wide test section. At inlet to the working section the turbulence level is around 0.4%, but a turbulence grid was placed at this location to generate turbulence at the VAWT test position of about 1%. A value of 1% turbulence intensity was used in this paper because it shows both positive performance at high TSR as well as very well defined vortices and stalling behaviour at low TSR. Too low turbulence intensity (0.4%) causes negative performance (CP) all throughout the range of TSR tested, whereas higher turbulence intensity (2.6%) suppressed the formation of a leading edge separation bubble that would eventually form into the dynamic stall vortex.

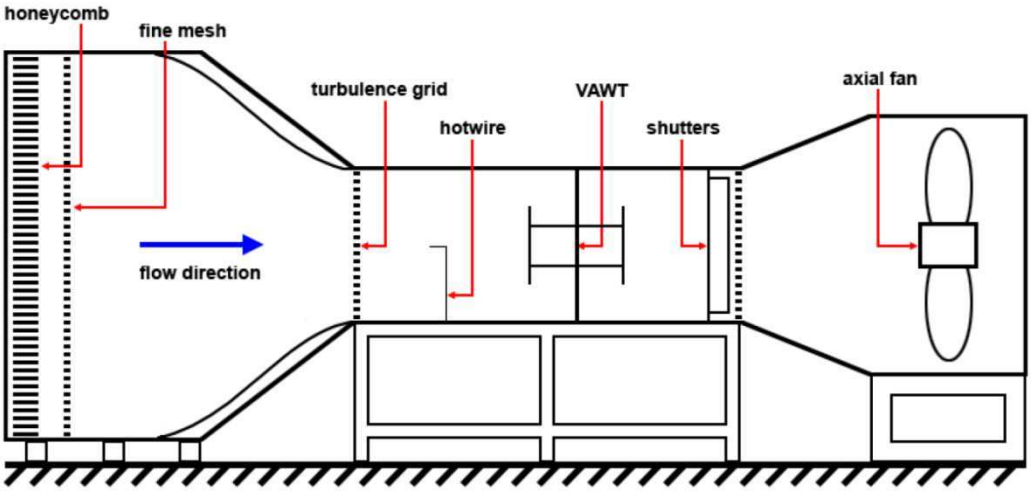

Figure 1. University of Sheffield wind tunnel facility with gust generators installed.

The tunnel was modified by the installation of shutters (downstream of the test section) which can be made to oscillate open and closed and generates the required unsteady wind velocities. These shutters can be held open and stationary for steady wind experiments. The shutters can be made to oscillate at different frequencies and different amplitudes. There are four slats on the right of the mechanism that close towards the right wall and another four on the left that close towards the left wall. This arrangement is chosen to avoid a biased lateral movement of the flow to one side of the tunnel, thereby minimising any unnecessary direct or indirect effects to the VAWT performance. A DC motor coupled to a 75:1 worm gear speed reducer drives a mechanism composed of bar linkages, cables and pulleys, and a pin–slot linkage.

Time resolved measurement of wind speed within the wind tunnel is carried out by a calibrated hot wire probe. The hot wire probe is calibrated in-situ with reference to a Furness Controls micro-manometer connected to a Pitot–static probe placed adjacent to the hot wire in the wind tunnel. These measurements are taken 20 rotor blade chords upstream of the turbine. Performance measurements from the turbine with and without the hot wire and Pitot probe present show that they have no effect on the performance of the turbine.

Wind Turbine Model

The VAWT used for this study is straight-bladed and mounted on a 25mm diameter central shaft running through the top and bottom walls of the test section where the bearings are located. The turbine is mounted in the centre of the test section cross section area but slightly downwind along the test section length. The turbine is based on three NACA0022 blades with chord c = 0.04m each supported by two support arms based on NACA0026 profiles (of 0.03m chord) at 25% and 75% rotor blade span positions. The rotor radius R is 0.35m and the blade span L is 0.6m giving the VAWT a solidity of $\sigma = 0.34$ following the conventional definition ($\sigma = Nc/R$, where N: number of blades). The turbine drive shaft is connected to a DC motor which provides the drive to spin the VAWT up to operating speed via an electromagnetic clutch. The drive shaft connected to Magtrol hysteresis brake to provide braking torque while a 3000–slot optical encoder provides a means to

measure rotational speed and its variation during a revolution. Torque is measured using a calibrated position based torque sensor.

It was not necessary to consider the effects of blockage in this investigation because absolute levels of performance were not important; only relative values of performance were needed as the paper's aim is to elucidate the flow physics present for the first time in an experimental setup.

Steady Blade CP

Measurement of the steady rotor blade power was carried out using an indirect method following a procedure developed by Edwards et al. [3]. The VAWT performance is first measured by allowing the rotor to spin down from a high rotational speed and the deceleration rate monitored using the optical encoder. For each test condition, two spin down tests are needed to determine the full performance of the rotor blades. The first involves the spin down of the rotor without the rotor blades but including the support arms. This is necessary to determine the system resistance which is always negative and includes the drag induced by the support arms as well as the bearings and hysteresis brake etc. It has been determined that the system resistance is independent of wind speed over the range tested here, i.e. the resistive torque curves from different spin down tests conducted at different wind speeds are identical [3]. The second spin down test is conducted with the rotor blades fitted and so measures the full turbine performance. For both spin down tests, the instantaneous torque is computed by multiplying the instantaneous rotational deceleration (ξ) by the rig's rotational moment of inertia (I_{rig}). The rotor blade torque is then the difference between the rotor torque (T_B) and the system resistance (T_{res}), see Equation 1. Instantaneous blade power is derived via Eq. 2. This system is used to determine the performance of the VAWT when it cannot self-sustain itself, i.e. the system resistance (due to bearing friction, and support arm drag) is greater than the torque developed by the rotor blades. For this particular turbine this usually occurs at wind speeds below 7m/s.

$$T_B + T_{res} + T_{app} = I_{rig}\xi \qquad \text{(Eq. 1)}$$

$$P_B = T_B\Omega \qquad \text{(Eq. 2)}$$

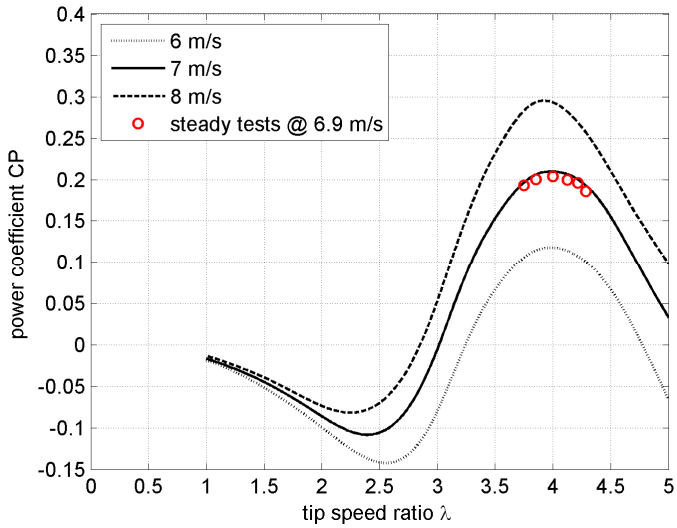

Figure 2. Steady torque results plotted over transient torque data.

The transient spin down method was shown by Edwards et al [3], to be a useful method of determining turbine CP. Since the technique is used again here in a modified form to determine the performance of the turbine with unsteady wind, further proof of the transient methods validity and accuracy are presented as performance coefficients in Figure 2. This shows the CP vs. λ for a wind speed of 7m/s, where the solid black line represents the data from the spin down method and the red circles represent the direct torque measurement of CP. It is clear that the results are well matched.

For tests at wind speeds of 7m/s and greater, the application of the hysteresis brake (T_{app}) is required to slow the turbine because positive rotor torque is developed which prevents the VAWT decelerating at these higher wind speeds (Reynolds numbers). Blade power is computed by subtracting both system resistance and brake applied from the rotor torque. The reader is referred to Edwards et al. [3] for the full details of the method including limitations and assumptions used. Maximum CP for 7m/s is around 21% and positive blade performance is observed between $\lambda = 3$ and $\lambda = 5$. The figure also indicates Reynolds number dependency of blade performance at this scale of the VAWT. Higher wind speeds result in higher CP and a wider λ band of positive performance, but for structural and safety reasons, spin down tests were conducted up to a maximum wind speed of 9m/s.

Measurement of Rotor Blade CP (Unsteady)

Measurement of the rotor blade CP of the VAWT running in unsteady wind requires a modification on the test procedure for the steady case presented above. The fundamental relationship of the torque terms involved is identical, see Eq. 1 and Eq. 2. The procedure for collecting the data for the unsteady wind experiments is complicated in practice, but simple in terms of data processing and is now described. Firstly, a steady wind speed is selected and the turbine operated at a constant rotational speed. The wind is then set fluctuating at the required amplitude and frequency by setting the required power input into the shutter drive mechanism. At this point some adjustment to the wind tunnel wind speed may be required to bring the mean wind speed back

to the required value. Once this is achieved, the turbine is now operating in unsteady wind conditions with the desired mean wind speed. This unsteady wind operation is continued for appropriately 10 minutes and until the turbine operates in a fully periodic manner i.e. periodic over a long time scale. Only after attaining periodicity are the turbine conditions measured. For each test condition, two minutes duration of data is logged, which equates to approximately 29 cycles of the wind fluctuation at its slowest rate. It was determined that ensemble averaging the data over this number of 30 of the wind variation gave the best quality results. It should be noted that the hysteresis brake applies a constant torque independent of rotational speed of the turbine. The data measured is the fluctuating variation with time of the rotor speed as recorded by the 3000 slot per rotation optical encoder. It is then possible to use this RPM variation with time to calculate the rotational acceleration of the turbine (ξ) with time and determine the instantaneous torque developed by the turbine. The resistive torque was determined during the first spin down tests and the combination of these measurements allows the determination of the rotor blade performance.

III. Experiment Results

The Reference Case.

Tests conducted at Ω_{mean} = 791 rpm ($\lambda \sim 4$) were used as a reference case as this is very near to the optimum λ of the steady wind performance curve. With the present test parameters (R = 0.35m, f_c = 0.46Hz, V_∞ = 6.97m/s) this resulted in the wind turbine executing 29 revolutions for one period of the wind speed fluctuation. The wind gust length scale is an order of magnitude larger than the rotor diameter implying that the wind turbine should be able to physically resolve the structures containing the majority of the unsteady energy within the wind cycle [15]. However, this does not imply that the turbine will be able to track the optimum λ as the wind fluctuates, it is only argued that the available energy in the unsteadiness is 'visible' to the VAWT and with the appropriate control system the VAWT will be able to extract much of the energy contained within the gust. Many VAWTs are small machines without complex control systems and so will operate in a manner similar to the turbine used here. If a turbine were to be operated at constant RPM the λ would of course still vary with the wind speed and in this case the torque what would have to be continuously varied to absorb the changes in power in the wind. The Sheffield 0022 turbine operates with constant applied torque and the RPM varies.

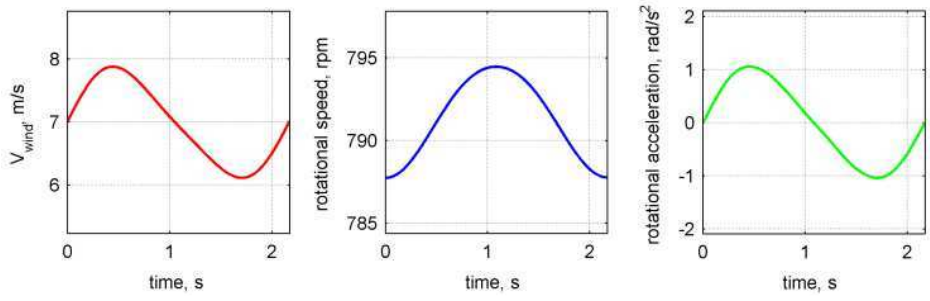

a. b. c.

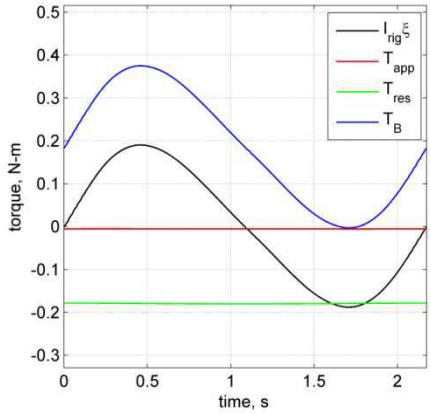

d.

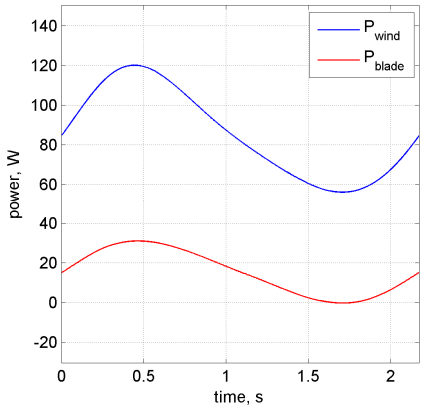

e.

Figure 3. Unsteady kinetics of the VAWT: a) wind velocity, b) RPM, c) acceleration, d) torque terms for one cycle, and e) wind power and blade power.

A wind turbine with low moment of inertia is desired so as to reduce the need for highly sensitive measurement sensors and transducers thus allowing the VAWT to be able to respond sufficiently enough to make measurements a possibility. The current VAWT has a rotational mass moment of inertia about the VAWT axis equal to 0.1805kg–m^2. This is slightly high for a VAWT of this scale but is unavoidable because of the construction techniques required to manufacture this turbine. Despite this inertia, the current instrumentation allows for the detection of less than 1 rpm change in rotational speed and as such this measurement resolution is perfectly acceptable.

As can be seen from Figure 3a, the profile of the fluctuating wind is a distorted sine wave. The positive fluctuation of the cycle is slightly shorter than the negative section because the latter involves the closing of the shutters against the wind. The power supply for the shutter drive responds to this resistance by increasing the input current while maintaining a constant voltage and in the absence of a full control system on the speed of rotation of the drive causes this skewed unsteady wind profile. Despite the lack of control system for the shutter mechanism, the resulting fluctuating cycle is very close to the desired sinusoidal shape and most importantly it is periodic.

The fluctuating rpm of the wind turbine shows a π phase lag from the wind, Figure 3a and 3b. The peak of the rpm occurs half way in the cycle where the wind speed is close to the mean value. The lowest point in the rpm cycle is at the beginning and end of the cycle where the wind speed is also close to the mean value. This behaviour suggests that there is little time delay in the response of the VAWT to the fluctuating wind. This is to be expected given the rotational frequency of the turbine is so much higher than that of the wind fluctuation frequency. An inspection of the acceleration shows that the peak and trough of the acceleration coincide with the wind speed maximum and minimum quite well. The distortion in the acceleration curve is also similar to that of the wind profile. When the acceleration of the VAWT is highest, this corresponds to the point of maximum wind speed and the steepest positive slope in the rpm curve. On the other hand, the lowest point in the acceleration curve coincides with the point of lowest wind speed and steepest negative slope in the rpm curve. Therefore the response of the VAWT to the changing wind is considered to be almost instantaneous.

The rotor torque $I_{rig}\xi$, which is the net torque, varies with respect to zero (Figure 3d). Positive acceleration produces positive rotor torque and reaches maximum at 0.19N·m. As the wind speed drops to the second half of the cycle, the acceleration plunges to the negative region resulting to negative net torque on the rotor. For the case shown, the applied torque T_{app} is zero while the resistive torque T_{res} is constant at –0.18 N·m. A point to note is the dependence of the resistive torque on the rotor rpm and while the rpm is fluctuating with the wind, the amplitude of the rpm fluctuation is very small compared to the magnitude of its mean value. The resistive torque corresponding to the changing rpm has a standard deviation of 7e–04N·m hence a constant resistive torque is observed. Solving for the blade torque T_B from Eq. 1 essentially pushes the net torque upward by an amount equal to the resistive torque T_{res}. The unsteady blade power is computed using the known blade torque T_B and rotational speed. Maximum blade power is 31.04W while the minimum is close to zero at –0.27W. The unsteady wind power can easily be derived. Maximum wind power is computed to be 120.11W while the minimum is 56.13W. Figure 3e shows the plots for the blade power and the wind power in one fluctuation cycle. The cycle average wind power was mentioned earlier to be 85.44W while the cycle average blade power is 15.35W. The power coefficient of the VAWT over one wind cycle is 0.18.

$$CP=\frac{P_B}{P_w}=\frac{T_B\omega}{\frac{1}{2}\rho A V_\infty^{\,3}} \qquad \text{(Eq. 3)}$$

The unsteady tip speed ratio λ is the instantaneous relationship between the rotational speed and the wind speed. When plotted against time, the unsteady λ curve is a mirror image of the unsteady wind profile (Figure 4a). This suggests λ is more sensitive to wind speed changes than to rotational speed variation. As the wind speed fluctuates to the positive peak, the λ drops from 4.11 at the start of the cycle to 3.68 close to the point of maximum wind speed. It does not occur at the point of maximum wind speed because the changing rpm also contributes to the unsteady λ and the relationship is non–linear. After reaching minimum value, λ steadily rises as the wind speed drops to the lowest magnitude. Close to the lowest point of the wind speed cycle λ attains its maximum value of 4.74.

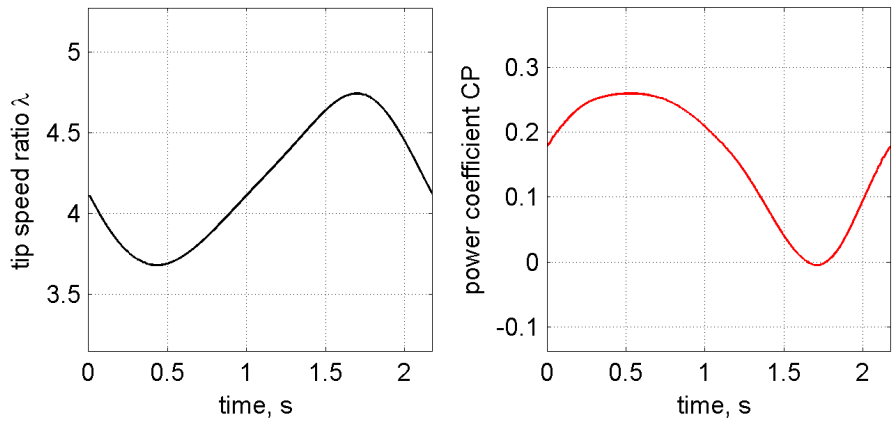

a. b.

Figure 4. Unsteady performance of the VAWT vs. time: a) λ, b) CP.

From Eq. 3, the CP is dependent on two fluctuating parameters: wind speed and rpm. The 180° phase difference of the rpm relative to wind speed does not make the relationship straightforward. The performance of the VAWT (Figure 4b) is highly dependent on the interaction of the two parameters and this makes the analysis more complicated. Although the profile of the wind speed variation is periodic and sinusoidal, the available wind power is a function of its cube. However, the blade power is a function of the rotational acceleration derived from the fluctuating rpm. Additionally, wind power varies with larger amplitudes and has a substantially higher mean compared to blade power. This induces a unique variation in the CP as the wind speed fluctuates. During the first half of the wind cycle where the speed changes from the mean to the maximum value and back, the CP is observed to rise gradually and flattens out early on before coming back to near its value at the start of the cycle. Conversely the behaviour of the CP in the second half of the cycle is sudden and steep with a deep trough at the point of lowest wind speed. Afterwards, the CP rises rapidly and attains higher values as the wind speed recovers to its mean state. From Figure 4b, one can see an increase in CP as the wind speed rises. From the start of the cycle where the CP is 0.18, the performance rises and slowly tapers off to a maximum of 0.26 after which drops to 0.19 midway in the cycle. At the start of the second half of the cycle, the drop in the value of the CP is observed to be faster than the section that just preceded it and eventually ends with a value of zero before rising again to 0.18 as the wind cycle is completed. When compared to the increase in CP of 0.08 in the first half of the cycle, the decrease of the CP in the second half is more than double at 0.19. The peak and trough of the unsteady CP curve are consistent to the maximum and minimum of the wind speed profile suggesting a Reynolds number dependence of the CP.

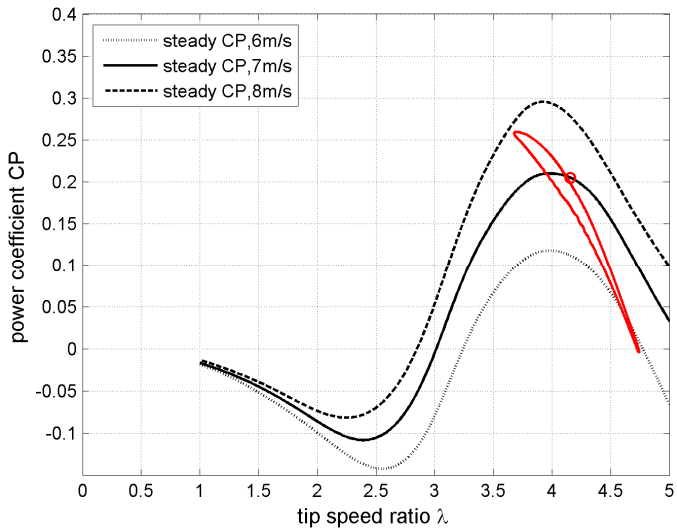

Figure 5. Unsteady wind performance versus steady wind performance.

A further inspection of this behaviour is carried out by overlaying the unsteady CP of the VAWT over steady CP curves at different wind speeds (Figure 5). One can see that the unsteady CP does not trace the steady performance curve of the VAWT at 7m/s. The unsteady curve cuts across the steady CP curves as the performance fluctuates with the changing wind. This is a very different observation compared to similar work

by McIntosh et al [9] and Scheurich and Brown [14] on a larger VAWT scale. Both numerical studies show that the performance of a 5kW VAWT in unsteady wind closely tracks the steady CP curve when the mean λ is higher than the optimum λ. A possible explanation for this is the difference in Reynolds number between the large scale VAWT and the wind tunnel scale VAWT. From a value of 0.18 at the start of the cycle, the unsteady CP increases with the wind and approaches the steady CP curve for 8m/s. The subsequent drop in wind speed does not cause the CP to follow the same path but trace a new one with slightly higher values. The small hysteresis loop in the unsteady CP implies slight dynamic stalling of the blades as they see more rapidly changing relative velocities and tip speed ratios than steady wind conditions. As a reference point, the equivalent steady CP of the VAWT at the mean rpm is 0.205 while the instantaneous CP at two points in the unsteady curve with the same λ value are both lower and the cycle average CP is also lower. When the wind speed reaches is lowest value in the cycle, the unsteady CP is already lower than the 6m/s steady CP curve even though the actual wind speed is still higher at 6.1m/s.

Effect of Varying the Mean λ

The performance of the VAWT in unsteady wind is further investigated by changing the mean λ while preserving the unsteady profile of the wind. This is accomplished by applying the brake on the VAWT to increase the resistive forces and reduce the mean rpm of the rotor. The plots of the fluctuating wind speed for the two different mean λ cases are shown in Figure 6a. There is a difference in the observed period of fluctuation between the two. The reference case with the higher mean λ has a period of t = 2.17s (f_c = 0.46Hz) while the case with the lower mean λ has a period of t = 1.91s (f_c = 0.52Hz). The difficulty in controlling the experiment parameters with their inter–dependent properties implies that the unsteady wind profiles cannot be matched precisely when run settings are changed. Nevertheless, the dissimilarity in periods is considered small when compared to the overall effect of the magnitude of the fluctuating wind speed. The mean wind speeds for both cases are very close at 6.97m/s for λ_{mean} = 4.1 and 6.96m/s for λ_{mean} = 3.8. The amplitudes of fluctuation are also very similar at 0.88m/s for λ_{mean} = 4.1 and 0.81m/s for λ_{mean} = 3.8, just more than 12% of the V_{mean}.

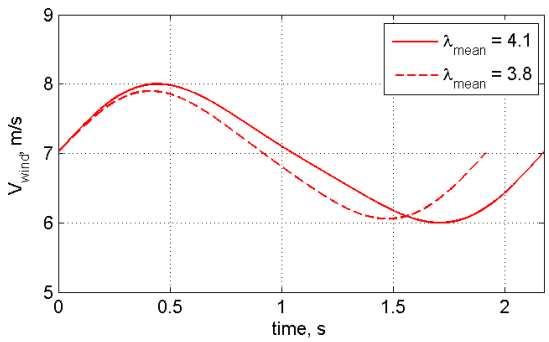

a.

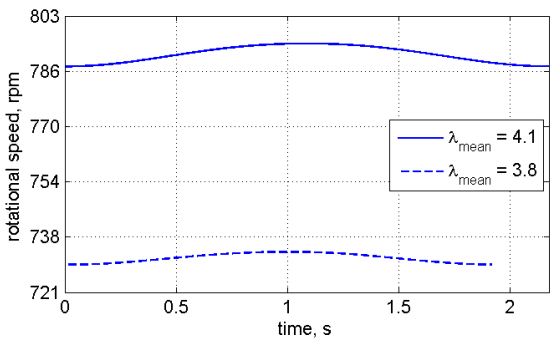

b.

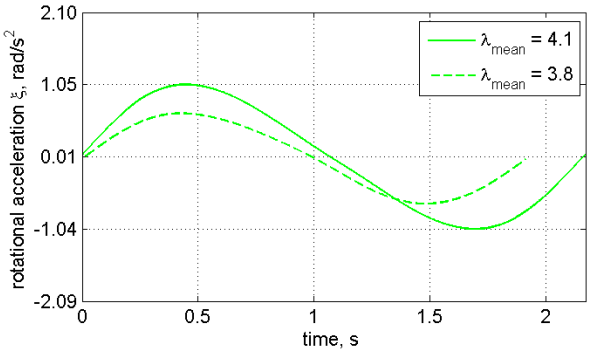

c.

Figure 6. Unsteady kinematics for different mean λ: a) wind velocity, b) RPM, c) acceleration.

Shown in Figure 6b is the plot of the unsteady rpm for the two cases. The mean rpm is 791rpm for λ_{mean} = 4.1 while it is 731rpm for λ_{mean} = 3.8. The resistive torque corresponding to these cases are 0.18N·m and 0.165N·m, respectively. From the torque equation (Eq. 1), this suggests a lower vertical shift of the blade torque T_B for λ_{mean} = 3.8 from the initial rotor torque $I_{rig}\xi$ position. However, there is an additional brake torque T_{app} of 0.03N·m for λ_{mean} = 3.8 that is not present in λ_{mean} = 4.1. This pushes the T_B curve of λ_{mean} = 3.8 closer, but still lower, to that of λ_{mean} = 4.1.

It can be seen that the peak–to–peak value of the rpm fluctuation is 6.73rpm for λ_{mean} = 4.1 and 3.77rpm for λ_{mean} = 3.8. The difference, which is almost double, greatly affects the computed rotational acceleration of the VAWT. More gentle slopes in rpm for λ_{mean} = 3.8 mean lower values of acceleration while larger amplitudes as in the case of λ_{mean} = 4.1 result to higher magnitudes of acceleration (Figure 6c). Since blade torque T_B is directly proportional to acceleration, the λ_{mean} = 4.1 case generates greater torque variation than the λ_{mean} = 3.8 case. The amplitudes of fluctuation of λ for the two cases are noticeably different as seen in Figure 7a. The amplitude for λ_{mean} = 4.1 is 0.53 while it is 0.46 for λ_{mean} = 3.8. Since the wind speed variation between cases do not vary much, λ is now dependent only on the rpm fluctuation. With the observed lower peak–to–peak variation of rpm in λ_{mean} = 3.8, the same can be expected on fluctuating λ with a lower peak–to–peak value.

The behaviour of the time varying CP cannot be simplified in the same manner. Both cases show a gradual rise and tapering off in CP during the first half of the wind cycle but a steep and sudden drop in the second half (Figure 7). From the start of its cycle, λ_{mean} = 4.1 gains 0.08 in CP from 0.18 to 0.26 before dropping to 0.19 as the first half of the cycle ends. However, the CP continues to drop and loses more than 0.19 of its value to less than zero. Similarly, λ_{mean} = 3.8 exhibits an initial slow rise in CP of 0.04 from 0.17 to a peak value of 0.21 and a subsequent deep trough in the second half with a loss of 0.1 from 0.19 to the lowest value of 0.09. The preceding observations point to a negative bias in CP variation even in a symmetrically fluctuating wind. There is more negative effect in performance despite constant energy content in the wind suggesting that unsteady wind is detrimental to the overall VAWT performance.

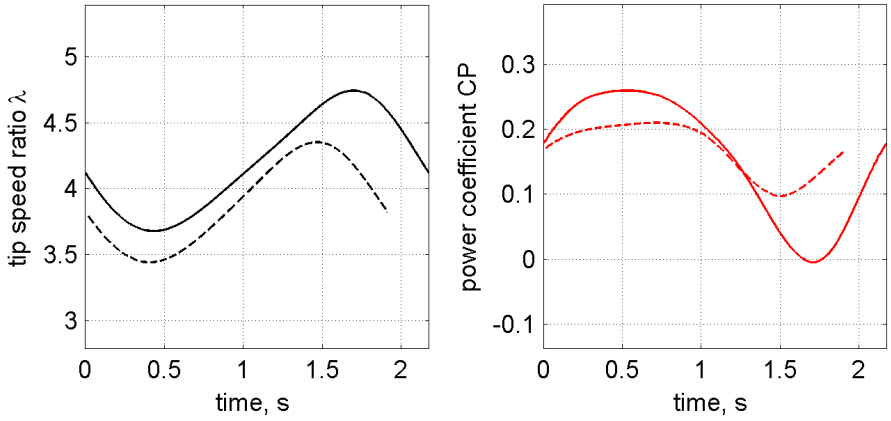

a. b.

Figure 7. Unsteady performance of the VAWT for the two λ cases: a) λ, b) CP.

The unsteady CP variation of the two λ cases is plotted against λ in Figure 8. Compared to λ_{mean} = 4.1, the unsteady CP of λ_{mean} = 3.8 shows a large hysteresis loop which further supports the argument that it is not possible to trace the unsteady performance of a micro–scale VAWT on steady CP curves. The hysteresis indicates the presence of deep stall, a phenomenon that is likely to occur at λ below the optimum performance point. Similarly, McIntosh et al [9] investigated a variety of mean λ and found that hysteresis loops in CP are formed when λ_{mean} is close to the optimum λ. However, the similarity ends there. McIntosh et al have seen a significant increase in the cycle CP of the VAWT especially at higher f_c whereas this study sees the opposite.

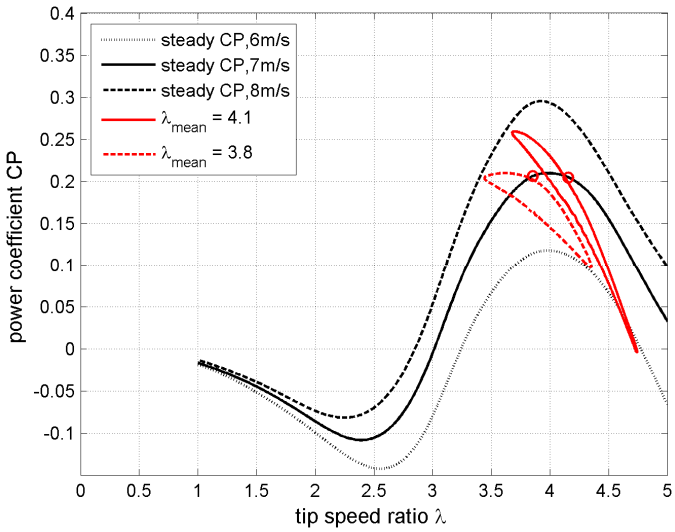

Figure 8. Unsteady performance of the VAWT at different mean λ.

The unsteady CP moves between different steady CP curves clearly showing Reynolds number dependency at this scale. Both cases illustrate a trend in the band of unsteady performance. The VAWT CP is expected to fluctuate from one steady CP curve to another depending on the amplitude of the fluctuating wind. For the cases considered, the amplitude is around 0.9m/s hinting that the CP should fluctuate between the 6m/s and 8m/s steady CP curves. The cycle CP for both cases is 0.18 while the steady wind CP counterparts are just above 0.20.

Effect of Varying the Fluctuation Amplitude

The influence of varying the amplitude of fluctuation was also investigated. Achieving this necessitated the changing of the closing angle of the shutters to change the flow restriction in the downwind of the test section. As with changing any test parameters from the reference test case, difficulty was encountered in trying to change only one setting without significantly affecting other settings. To achieve the same mean wind speed while having smaller amplitude, getting the same period of fluctuation was inevitably going to be difficult. The new case with the smaller amplitude fluctuation V_{amp} = ±7% has a period of t = 1.87s (f_c = 0.54Hz) (Figure 9a). This is close to the λ_{mean} = 3.8 case of the previous section and not too far from the reference case V_{amp} = ±12% of t = 2.17s (f_c = 0.46Hz). The mean wind speed for V_{amp} = ±7% is 6.87m/s, a slight drop from the 6.97m/s wind speed for V_{amp} = ±12%. The 0.1m/s difference between mean values is deemed small since its effect on the wind power is only a 3.5W drop, about 4% power reduction. The amplitude of wind fluctuation for V_{amp} = ±7% is approximately 7% of the V_{mean} at 0.47m/s.

There is a very small difference in the rotational speed profiles between the two cases. As reported in the previous section, the mean rotational speed Ω_{mean} for V_{amp} = ±12% is 791rpm. On the other hand Ω_{mean} = 795rpm for V_{amp} = ±7%, a mere 0.5% difference. In terms of the resistive torque corresponding to these rpm levels, T_{res} = 0.18N·m for both V_{amp} = ±7% and V_{amp} = ±12%. An expected outcome is the difference in the peak–to–peak value of the rpm fluctuation (Figure 9b). For V_{amp} = ±7% this turns out to be 3.58rpm, which is about half of the value for V_{amp} = ±12%. The smaller peak–to–peak results to a similar outcome in rotational acceleration as the λ_{mean} = 3.8 case where the gentler slopes in the rpm profile cause smaller magnitudes in rotational acceleration (Figure 9c). Consequently, the magnitudes of the unsteady torque are much smaller than the reference case. The mean λ is 4.2 for V_{amp} = ±7%, slightly higher than λ_{mean} = 4.1 for V_{amp} = ±12%. This is to be expected because for the V_{amp} = ±7% case, Ω_{mean} is a little higher and V_{mean} is a bit lower. Additionally the amplitude of λ fluctuation is smaller as a direct consequence of the smaller amplitude of the unsteady wind (Figure 10a).

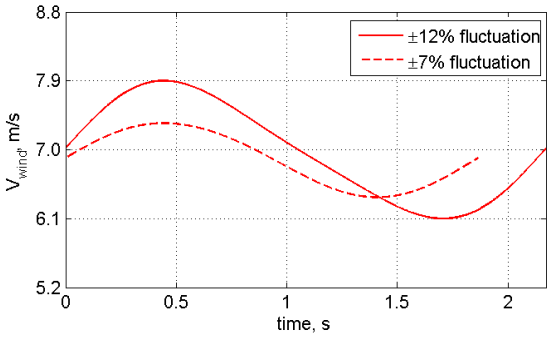

a.

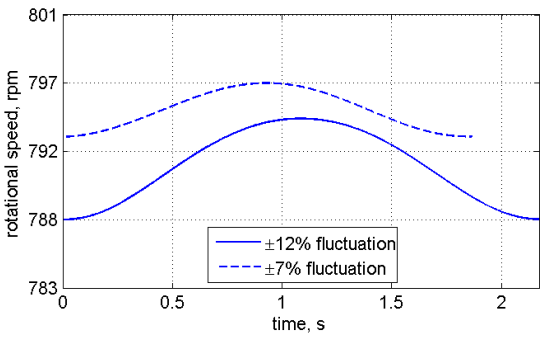

b.

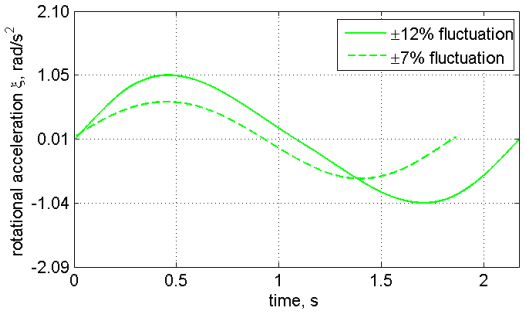

c.

Figure 9. Unsteady kinematics for different V_{amp}: a) wind velocity, b) RPM, c) acceleration.

The variation of the CP versus time when V_{amp} = ±7% is similar to the previous cases investigated (V_{amp} = ±12% at λ_{mean} = 4.1 and λ_{mean} = 3.8). As already seen in the previous section where a bias towards the negative performance is observed, such observation is also true with a smaller amplitude of fluctuation (Figure 10b). At the start of the cycle, the instantaneous CP is 0.204 and gradually rises to a peak value of 0.257. The subsequent fall of the wind speed causes the CP to follow suit and return to a value close to the initial CP at 0.197. As the wind speed continues to drop to the minimum, the CP also decreases until it reaches its lowest at 0.099. Between the initial CP and the maximum, the increase in CP is 0.053. However, the drop in CP between the initial value and the minimum is almost double at 0.105. The results are consistent to the previous test cases where the overall cycle CP is reduced when the VAWT is subjected to unsteady wind conditions.

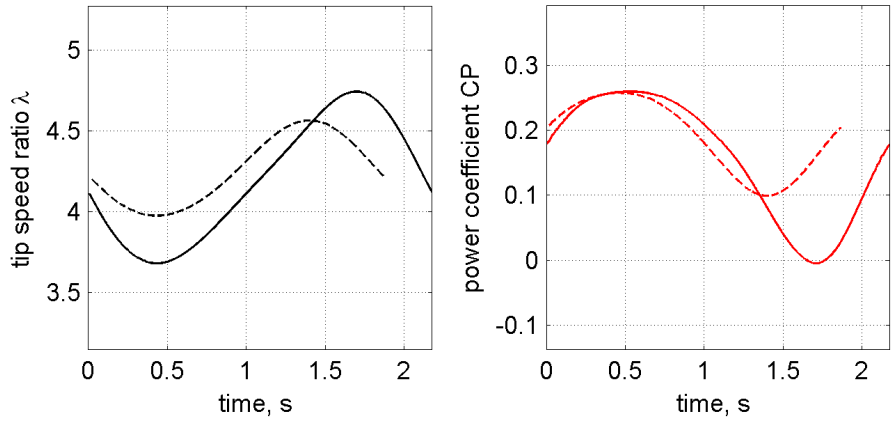

a. b.

Figure 10. Unsteady performance of the VAWT for the two V_{amp} cases: a) λ, b) CP.

Figure 11 shows the unsteady CP plotted against λ. Noticeably the path that the CP traces does not form a hysteresis loop. This is expected since the wind speed amplitude is small enough that deep stalling is suppressed at these operating λ. Scheurich and Brown [14] observe a similar trend in the CP curve with varying amplitudes. In their investigation, a fluctuation amplitude of ±30% induces hysteresis in the unsteady CP while a ±10% amplitude does not. The unsteady λ barely drops below the optimum λ value. When the VAWT is operating at these conditions, the blade stall behaviour is similar to a very slowly pitching aerofoil in constant free stream. The separation starts from the trailing edge and moves up towards the leading edge. A leading edge separation bubble never forms and most of the time only partial stall is seen. The path of the

unsteady CP is also comparable to the previous results where the curve cuts across the steady CP curves approach the adjacent curves as the wind speed fluctuates to its extreme values. The cycle CP for V_{amp} = ±7% is 0.18, a 0.01 drop from the steady CP value of 0.19.

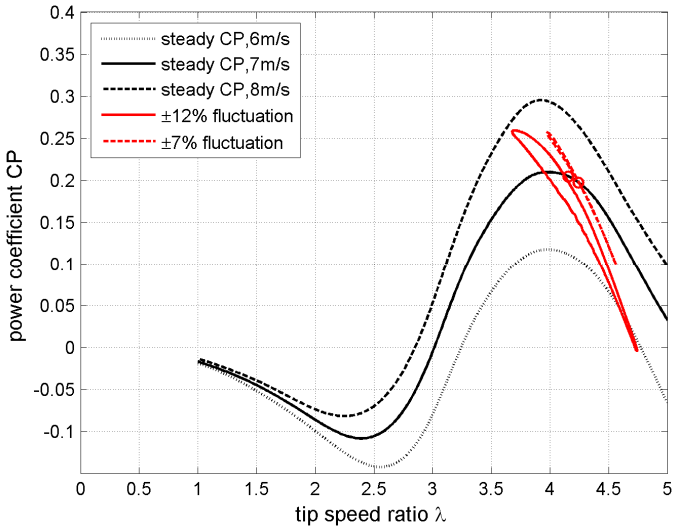

Figure 11. Unsteady performance of the VAWT at different V_{amp}.

VI. Conclusions

Unsteady wind experiments have shown that unsteady VAWT performance does not follow steady CP curves. For the mean wind speed of V_{mean} = 7m/s, the instantaneous CP rises and approaches the steady CP profile of a higher V_{∞} as the wind speed increases. The maximum unsteady CP is 0.26 and is greater than the maximum CP in steady wind. The fall of CP from the mean to its lowest value causes the CP to fall and move towards the steady CP profile of 6m/s. The cycle average CP of the VAWT is lower at 0.18 compared to the steady CP value of 0.205 at the corresponding λ.

Lowering the λ_{mean} from 4.1 to 3.8 still shows the unsteady CP-λ profile to cut across steady CP curves. However, the unsteady CP profile now shows a large hysteresis that drastically affects the overall performance of the VAWT despite the minimum CP falling to only 0.09 versus the reference case minimum of just below zero. The cycle CP of the λ_{mean} = 3.8 case is equal to the reference case at 0.18.

When the amplitude of fluctuation V_{amp} is changed instead, a similar deterioration of performance is measured. The extents of the unsteady CP profiles are much shorter than the reference case when the V_{amp} is reduced from ±12% to ±7%. No visible hysteresis in the CP is seen and the reduction in cycle CP is much less from the steady CP value of 0.19 to the unsteady cycle CP of 0.18.

All in all, unsteady free stream causes a drop in performance of the laboratory scale VAWT tested.

Acknowledgements

For the funding provided for this research, Mr.Eboibi would like to thank the Education Trust Funds (ETF) of Nigeria through the Delta State Polytechnic, Ozoro and Mr.Danao would like to thank the Engineering Research and Development for Technology Program of the Department of Science and Technology through the University of the Philippines College of Engineering.

References

[1] Bertenyi, T., Wickins, C., and Mcintosh, S. C., 2010, "Enhanced Energy Capture through Gust-Tracking in the Urban Wind Environment," 48th AIAA Aerospace Sciences Meeting Including the New Horizons Forum and Aerospace Exposition, Orlando, Florida.

[2] Dixon, K., Simao Ferreira, C. J., Hofemann, C., Van Brussel, G. J. W., and Van Kuik, G., 2008, "A 3d Unsteady Panel Method for Vertical Axis Wind Turbines," European Wind Energy Conference & Exhibition (EWEC) 2008, eds. Brussels, pp. 1-10.

[3] Edwards, J. M., Danao, L. A., and Howell, R. J., 2012, "Novel Experimental Power Curve Determination and Computational Methods for the Performance Analysis of Vertical Axis Wind Turbines," Journal of Solar Energy Engineering, 134(3), pp. 11.

[4] Simão Ferreira, C. J., Van Brussel, G. J. W., and Van Kuik, G., 2007, "2d Cfd Simulation of Dynamic Stall on a Vertical Axis Wind Turbine: Verification and Validation with Piv Measurements," *45th AIAA Aerospace Sciences Meeting and Exhibit*, Reno, Nevada.

[5] Mertens, S., Van Kuik, G., and Van Bussel, G., 2003, "Performance of an H-Darrieus in the Skewed Flow on a Roof," Journal of Solar Energy Engineering, 125(4), pp. 433-440.

[6] Simão Ferreira, C. J., Van Kuik, G., and Van Brussel, G. J. W., 2006, "Wind Tunnel Hotwire Measurements, Flow Visualisation and Thrust Measurements of a Vawt in Skew," 44th AIAA Aerospace Sciences Meeting and Exhibit, Reno, Nevada.

[7] Balduzzi, F., Bianchini, A., Carnevale, E. A., Ferrari, L., and Magnani, S., 2012, "Feasibility Analysis of a Darrieus Vertical-Axis Wind Turbine Installation in the Rooftop of a Building," Applied Energy, 97(0), pp. 921-929.
[8] Mcintosh, S. C., Babinsky, H., and Bertenyi, T., 2007, "Optimizing the Energy Output of Vertical Axis Wind Turbines for Fluctuating Wind Conditions," 45th AIAA Aerospace Sciences Meeting and Exhibit, Reno, Nevada.
[9] Mcintosh, S. C., Babinsky, H., and Bertenyi, T., 2008, "Unsteady Power Output of Vertical Axis Wind Turbines Operating within a Fluctuating Free-Stream," 46th AIAA Aerospace Sciences Meeting and Exhibit, Reno, Nevada.
[10] Hayashi, T., Hara, Y., Azui, T., and Kang, I.-S., 2009, "Transient Response of a Vertical Axis Wind Turbine to Abrupt Change of Wind Speed," Proceedings of the European Wind Energy Conference and Exhibition, Marseille, France.
[11] Kooiman, S. J., and Tullis, S. W., 2010, "Response of a Vertical Axis Wind Turbine to Time Varying Wind Conditions Found within the Urban Environment," Wind Engineering, 34(4), pp. 389-401.
[12] Danao, L. A., and Howell, R., 2012, "Effects on the Performance of Vertical Axis Wind Turbines with Unsteady Wind Inflow: A Numerical Study," 50th AIAA Aerospace Sciences Meeting including the New Horizons Forum and Aerospace Exposition, Nashville, Tennessee.
[13] Hara, Y., Hara, K., and Hayashi, T., 2012, "Moment of Inertia Dependence of Vertical Axis Wind Turbines in Pulsating Winds," International Journal of Rotating Machinery, 2012(2012), pp. 12.
[14] Scheurich, F., and Brown, R. E., 2012, "Modelling the Aerodynamics of Vertical-Axis Wind Turbines in Unsteady Wind Conditions," Wind Energy, pp. 17.
[15] Mcintosh, S. C., 2009, "Wind Energy for the Built Environment," Ph.D. thesis, Cambridge University, Cambridge.